

This discussion paper is/has been under review for the journal Ocean Science (OS).
Please refer to the corresponding final paper in OS if available.

Towards high resolution mapping of 3-D mesoscale dynamics from observations: preliminary comparison of retrieval techniques and models within MESCLA project

B. Buongiorno Nardelli^{1,2}, S. Guinehut³, A. Pascual⁴, Y. Drillet⁵, S. Ruiz⁴, and S. Mulet³

¹Istituto di Scienze dell'Atmosfera e del Clima, Roma, Italy

²Istituto per l'Ambiente Marino Costiero, Napoli, Italy

³CLS-Space Oceanography Division, Ramonville Saint-Agne, France

⁴IMEDEA(CSIC-UIB), Esporles, Spain

⁵Mercator Océan, Ramonville Saint-Agne, France

Received: 1 March 2012 – Accepted: 4 March 2012 – Published: 14 March 2012

Correspondence to: B. Buongiorno Nardelli (bruno.buongiornoardelli@cnr.it)

Published by Copernicus Publications on behalf of the European Geosciences Union.

OSD

9, 1045–1083, 2012

**High resolution
mapping of 3-D
mesoscale dynamics**

B. Buongiorno Nardelli et
al.

Title Page

Abstract

Introduction

Conclusions

References

Tables

Figures

⏪

⏩

◀

▶

Back

Close

Full Screen / Esc

Printer-friendly Version

Interactive Discussion



Farneti et al., 2010; and references therein). In fact, significant variations in the vertical exchanges could cause a reduction of the atmospheric CO₂ absorption and sequestration in the deep ocean, as well as a decrease in nutrient availability for phytoplankton growth and reduced sinking of organic matter (biological pump). These variations might thus have an impact on global climate and marine ecosystem. In turn, it is still not fully assessed how mesoscale activity and associated vertical motions are influenced by observed interannual/climatic changes.

In this context, the main MESCLA objective is the analysis of the interannual variability of the vertical exchanges associated to mesoscale dynamics, from a combination of observations and models. However, while the vertical component of ocean currents can be diagnosed in primitive equation numerical models by solving the continuity equation, the same technique is not applicable to direct observations. This is due, on one hand, to the few current measurements available, and, on the other hand, to the high error that would result from the computation of the divergence from measured horizontal velocities, that may include significant instrumental errors. It is also clearly impossible to use the continuity equation to estimate the vertical velocities from dynamic heights (computed from temperature and salinity profiles), as the geostrophic velocities are non-divergent by definition. On the other hand, simplified diagnostic models can be applied to retrieve the vertical velocity field from three-dimensional (3-D) estimates of geostrophic currents and density fields (e.g. Tintoré et al., 1991; Allen and Smeed, 1996; Buongiorno Nardelli et al., 2001; Pascual et al., 2004; Ruiz et al., 2009). Nevertheless, it must be stressed that sufficiently high spatial resolution must be reached to obtain accurate estimates of the vertical exchanges from 3-D observation-based systems. In fact, in order to correctly retrieve the vertical velocities associated with mesoscale features, one should be able to resolve very small scales, i.e. up to less than 10 (for a complete review on the topic, see Klein and Lapeyre, 2009). Actually, 3-D observation-based systems are far enough from being able to correctly reproduce the global variability at these scales (Willis et al., 2003; Roemmich and Gilson, 2009; Von Schuckmann et al., 2009; Guinehut et al., 2004, 2012; Larnicol et al., 2006). In

High resolution mapping of 3-D mesoscale dynamics

B. Buongiorno Nardelli et al.

[Title Page](#)[Abstract](#)[Introduction](#)[Conclusions](#)[References](#)[Tables](#)[Figures](#)[Back](#)[Close](#)[Full Screen / Esc](#)[Printer-friendly Version](#)[Interactive Discussion](#)

High resolution mapping of 3-D mesoscale dynamics

B. Buongiorno Nardelli et al.

Title Page

Abstract

Introduction

Conclusions

References

Tables

Figures



Back

Close

Full Screen / Esc

Printer-friendly Version

Interactive Discussion

this framework, the first step of MESCLA project was the improvement of the existing MyOcean observation-based products (namely MyOcean ARMOR3D, Guinehut et al., 2012) and the development and test of new high resolution horizontal interpolation and vertical extrapolation techniques (Buongiorno Nardelli, 2012; Buongiorno Nardelli et al., 2006; Buongiorno Nardelli and Santoleri, 2004, 2005). As a second step, a quasi-geostrophic diagnostic numerical model (the Q-vector formulation of the Omega equation) has been used to estimate the vertical velocities (Pascual et al., 2004; Ruiz et al., 2009). The Omega equation was applied to different MyOcean products (both model and observation-based) in order to quantify the limitations in the diagnostic tools used and the impact of the resolution on the retrieved velocity. The preliminary results of these first two steps are the subject of the present paper.

The comparison of both model/assimilation and purely observation-based data is expected to provide a more robust analysis of mesoscale vertical velocity variability. In fact, the observation-based products are obtained through relatively simple statistical analyses and simple approximations. Conversely, it is evident that data assimilation into models allows to obtain more accurate analyses and forecasts, especially at the shorter time scales, but one must be aware of the fact that model results can be greatly influenced by the specific model configurations and by the uncertainties in the boundary condition imposed (e.g. atmospheric forcing used, parameterization of smaller scale processes, spatial resolution, etc.). Comparing the two approaches might thus help to better understand the vertical exchanges associated with mesoscale processes.

To summarize, in this paper we will thus describe:

- the strategies adopted to improve the observation-based products resolution, namely the ingestion of different high resolution Sea Surface Temperature level 4 products (SST L4, i.e. interpolated data) and of a high resolution Sea Surface Salinity product developed within MESCLA in the ARMOR3D processing (Sect. 4.1.1);

High resolution mapping of 3-D mesoscale dynamics

B. Buongiorno Nardelli et al.

Title Page

Abstract

Introduction

Conclusions

References

Tables

Figures

⏪

⏩

◀

▶

Back

Close

Full Screen / Esc

Printer-friendly Version

Interactive Discussion

- The implementation of new extrapolation methodologies to obtain experimental higher resolution 3-D re-analyses based on a high resolution Sea Surface Salinity product developed within MESCLA, on one selected high resolution SST L4 product (Sect. 4.1.2) and standard altimeter products;
- 5 – the diagnostic model used to retrieve the quasi-geostrophic vertical velocity field from the previously described observation-based density and geostrophic velocities fields (Sect. 4.2);
- a preliminary evaluation of the 3-D reconstruction methods performances (Sects. 5.1–5.2);
- 10 – the comparison of the MyOcean MERCATOR PSY3V2R2 and PSY2V3R1 model vertical velocities (see Sect. 3) with the quasi-geostrophic currents obtained from the model density field (Sect. 5.3);
- the impact of the increased resolution on the estimation of the vertical velocity field from the 3-D observation-based products (Sect. 5.4).

15 Given the lack of independent (direct) measurements of the vertical velocities, a full validation of the new products is clearly not possible. Consequently, the approach followed here relies on the comparison between several different products, concentrating on a well-known area of intense mesoscale activity (the Gulf Stream) and on a specific day (the 17 October 2007), and on the analysis of the impact of the new techniques
 20 on the vertical velocity field estimation. Additional investigations, including longer time series and more detailed dynamical analyses are left for future work.

2 Observations

Any vertical extrapolation method requires, on one hand, an historical in situ dataset to estimate the direct correlations between the parameters of interest (namely, temperature, salinity and steric height) or to identify their main statistical or empirical modes
 25

of variability, and, on the other hand, surface measurements of at least two of these parameters to be able to extrapolate their vertical profiles. In the following, the datasets used within MESCLA project are briefly described.

2.1 In situ data

5 The operational ARMOR3D and the experimental ARMOR3D-MESCLA systems (Sect. 4.1) are trained with the profiles of temperature (T) and salinity (S) coming from Coriolis/ARGO for more recent data (<http://www.coriolis.eu.org>), and from the EN3 dataset for the historical data (Ingleby and Huddleston, 2007). Similarly, the dataset used within MESCLA to test the new vertical extrapolation techniques mEOF-R consists of the quality controlled T and S profiles measured by ARGO and CTD sensors and distributed by the MyOcean In Situ Thematic Assembly Centre (more precisely, these are the profiles used by CORIOLIS In Situ Analysis System (ISAS) to produce their global temperature and salinity 3-D fields). The same dataset served also to develop the MESCLA high resolution SSS product (Buongiorno Nardelli, 2012). These observations are pre-processed according to ARGO recommendations for data quality control (Wong et al., 2012).

2.2 Surface data

2.2.1 SSS

20 The Sea Surface Salinity (SSS) L4 data used in input to the mEOF-R 3-D reconstruction (Sect. 4.1.2) was developed as an experimental product in the framework of MESCLA project. Its space-time resolution is $1/10^\circ$, daily. The method used to retrieve this SSS field is based on an Optimal Interpolation (OI) algorithm that interpolates in situ salinity including satellite high-pass filtered sea surface temperature (using $1/10^\circ$ ODYSSEA SST L4) in the determination of the weights used to interpolate SSS observations. The covariance function parameters (i.e. spatial, temporal and thermal

High resolution mapping of 3-D mesoscale dynamics

B. Buongiorno Nardelli et al.

Title Page

Abstract

Introduction

Conclusions

References

Tables

Figures

⏪

⏩

◀

▶

Back

Close

Full Screen / Esc

Printer-friendly Version

Interactive Discussion



decorrelation scales) and the noise-to-signal ratio have been determined empirically, as fully described in Buongiorno Nardelli (2012).

2.2.2 SLA/ADT

The altimeter Sea Level Anomalies (SLA) and Absolute Dynamic Topography (ADT) gridded data used for the 3-D retrieval are those produced and disseminated by the SSALTO/DUACS centre and represent the MyOcean Sea Level Thematic Assembly Centre intermediate product (AVISO, 2011). They are obtained as daily combined maps from all processed altimeters (currently: Jason-1, Jason-2 and Envisat for the NRT products) with a $1/3^\circ$ horizontal resolution.

2.2.3 SST

Different satellite SST datasets have been used for the different phases of the work, each characterized by different nominal and effective resolution (as summarized in Table 1). In fact, as discussed by Reynolds and Chelton (2010), the true resolution of a L4 product is given by a combination of the grid spacing and of the analysis procedures and configurations applied (e.g. weighting functions and background fields). As a consequence, while combined ARMOR3D product is based on the Reynolds Optimally Interpolated L4 SST both at low (1° , corresponding to MyOcean V0 product) and high ($1/4^\circ$, corresponding to MyOcean V1 product) resolution (Larnicol et al., 2006; Guinehut et al., 2012), the higher resolution tests on ARMOR3D system have been performed also on the ODYSSEA L4 data produced by Ifremer in the framework of the MERSEA project and maintained as part of MyOcean (Autret and Piollé, 2007), and on the Operational SST and Sea Ice Analysis system (OSTIA, see Donlon et al., 2011) also distributed as part of the MyOcean Sea Surface Temperature Thematic Assembly Centre. ODYSSEA provides daily SST estimates on a $0.1 \times 0.1^\circ$ grid for the Global Ocean, based on both infrared and microwave measurements, while OSTIA L4 is available on a $1/20^\circ$ horizontal grid and includes also in situ SST measurements.

High resolution mapping of 3-D mesoscale dynamics

B. Buongiorno Nardelli et al.

Title Page

Abstract

Introduction

Conclusions

References

Tables

Figures



Back

Close

Full Screen / Esc

Printer-friendly Version

Interactive Discussion



For the test of the new extrapolation techniques (Sect. 4.1.3), only the ODYSSEA L4 has been used. This choice was driven on one hand by the fact that ODYSSEA is among the highest resolution Global SST L4 available and quality controlled operationally (see also Dash et al., 2010), its algorithm is particularly able to retain the smaller spatial scale signals without smoothing too much the original observations (e.g. Maturi et al., 2010) and, on the other hand, by the fact that it is the same product used to retrieve the high resolution SSS by Buongiorno Nardelli (2012).

3 Model output

The model outputs used in this study are daily means computed from the global physical ocean forecasting system delivered as intermediate products by the global Monitoring and Forecasting Centre from MyOcean, namely Mercator Océan. In order to investigate the impact of the horizontal resolution in the vertical velocities reconstruction phase, the two components which compose the global system have been used: the global $1/4^\circ$ called PSY3V2R2 and the North Atlantic and Mediterranean Sea $1/12^\circ$ called PSY2V3R1 (Dombrowsky et al., 2009; Lellouche et al., 2012). Except the horizontal resolution, the two configurations are really close in term of ocean model version, numerical schemes, physical parameterizations, bathymetry, atmospheric forcing, assimilation scheme and assimilated data. The model configuration is based on NEMO1.09 (Madec, 2008) with vertical z coordinates including partial step parameterization and 50 vertical levels from 1 m resolution at the surface to 400 m at the bottom. The main numerical schemes used in these configurations are a TVD advection scheme and an isopycnal laplacian diffusion for the tracers, the energy and enstrophy conserving scheme and a biharmonic diffusion for the momentum. The vertical mixing scheme is TKE with an enhanced convection parameterization in case of instability of the water column. All these options are classical and used in global ocean model as mentioned in Barnier et al. (2006). The atmospheric forcing for the real time production is based on daily average of the atmospheric variables or flux

High resolution mapping of 3-D mesoscale dynamics

B. Buongiorno Nardelli et al.

Title Page

Abstract

Introduction

Conclusions

References

Tables

Figures



Back

Close

Full Screen / Esc

Printer-friendly Version

Interactive Discussion



provided by the ECMWF real time forecasting system. The assimilation scheme (Tranchant et al., 2008) used in both configurations is based on the SEEK filter which allows assimilation of the sea level along-track satellite observations delivered by the MyOcean sea level Thematic Assembly Centre., the temperature and salinity profiles from the MyOcean insitu Thematic Assembly Centre and the RTG sea surface temperature (http://polar.ncep.noaa.gov/sst/oper/Welcome.html). The model outputs used in this study are based on the “best analysis” which is performed every week with a one week delay in time to assimilate the most of observations over a one week assimilation window. This system was the global forecasting system operated during the V0 phase of MyOcean. The vertical velocity which is used as “reference” in this study to validate the quasi-geostrophic Omega equation is computed by an upward integration of the horizontal divergence from the bottom (Madec, 2008) which is the standard way to compute the vertical velocities in NEMO model in the case of a free surface condition.

4 Methods

4.1 3-D reconstruction

Several dynamic, variational, statistical and empirical techniques have been developed in the past to retrieve 3-D fields from a combination of in situ and satellite data (e.g. Carnes et al., 1994; Gavart and De Mey, 1997; Pascual and Gomis, 2003; Meinen and Watts, 2000; Watts et al., 2001; Mitchell et al., 2004). In fact, many of these methods are technically similar to some assimilation schemes (Optimal Interpolation-like), with the difference that the first guess used, i.e. the background analysis, is given by an average over the observations instead of a numerical model forecast. The error associated to this analysis thus represents the actual system variability. In essence, most statistical methods are based on the analysis of covariance relative to a set of in situ data profiles and on the identification of the principal modes characterizing the latter. However, the accuracy of each technique depends on the choice of the variables characterizing the

High resolution mapping of 3-D mesoscale dynamics

B. Buongiorno Nardelli et al.

Title Page

Abstract

Introduction

Conclusions

References

Tables

Figures



Back

Close

Full Screen / Esc

Printer-friendly Version

Interactive Discussion



state of the system, as well as the number of degrees of freedom which each method absorbs (e.g. Buongiorno Nardelli and Santoleri, 2004).

Univariate techniques such as single EOF (*Empirical Orthogonal Function*) Reconstruction analyze the principal components of each parameter along the water column and hypothesize a relationship between the amplitude of such components and a (not necessarily linear) combination of surface parameters (Carnes et al., 1994). Simpler methods, as the one used within ARMOR3D, assume a direct correlation between surface and deep values (Guinehut et al., 2012). The new methods considered within MESCLA are based on multivariate approaches (*Coupled Pattern Reconstruction-CPR; multivariate EOF Reconstruction, mEOF-r*). These methods analyze the steric height, temperature and/or salinity covariance and reconstruct the vertical profiles via a combination of a limited number of modes. Following an idea first proposed by Pascual et al. (2003), they include an approximation of the geopotential streamfunction (the steric height profile) in the status vector, thus more directly correlating physical-chemical parameter variability to dynamics. The application of these methods already yielded promising results, also compared to empirical methods such as the computation of the Gravest Empirical Modes (Buongiorno Nardelli and Santoleri, 2005).

Within MESCLA a double approach has thus been followed to improve the resolution of the observation-based 3-D fields. The two approaches involve different levels of complexity and might be considered as potential successive steps in a gradual improvement of operational products. As a first step, the algorithm used to obtain the MyOcean ARMOR3D product has been adapted to ingest higher resolution SST data. Then mEOF-R technique has then been adapted and tested on a subset of input data.

4.1.1 Increasing ARMOR3D spatial resolution

The combined ARMOR3D product is computed every week (Wednesday fields) on a $1/3^\circ$ Mercator horizontal grid, which corresponds to the altimeter SLA grid and from the surface down to 1500-m depth on 24 vertical levels. ARMOR3D method, thoroughly described in Guinehut et al. (2012) this same volume, consists in the improvement of

High resolution mapping of 3-D mesoscale dynamics

B. Buongiorno Nardelli et al.

Title Page

Abstract

Introduction

Conclusions

References

Tables

Figures



Back

Close

Full Screen / Esc

Printer-friendly Version

Interactive Discussion



High resolution mapping of 3-D mesoscale dynamics

B. Buongiorno Nardelli et al.

Title Page

Abstract

Introduction

Conclusions

References

Tables

Figures

⏪

⏩

◀

▶

Back

Close

Full Screen / Esc

Printer-friendly Version

Interactive Discussion

a climatological first guess using two main steps. At first, synthetic temperature (T) profiles are estimated by extrapolating altimeter and SST data through a multiple linear regression method and covariances computed from historical data. For synthetic salinity (S) profiles, the method uses only altimeter data. Successively, the synthetic profiles (hereafter referred to as *synthetic ARMOR3D* fields) are combined with in situ temperature and salinity profiles using an optimal interpolation method (Bretherton et al., 1976). These fields will be hereafter referred to as *combined ARMOR3D*.

As a preliminary step, ARMOR3D performs some crucial processing of altimeter data, being able to extract the steric contribution to the sea level variations consistent with the first 1500-m depth (filtering out the eustatic component and the deep steric contribution). This pre-processing is based on regression coefficients deduced from an altimeter/in situ comparison study (Guinehut et al., 2006; Dhomps et al., 2011).

In the present work, the three SST products described in Sect. 2 have been used to test the impact of SST resolution on the synthetic T field estimation (step one of the method). Additionally, the use of MESCLA experimental HR SSS fields has also been tested for the reconstruction of the synthetic salinity. While the synthetic ARMOR3D salinity fields is obtained with a simple linear regression to altimeter SLA, the method has been modified to a multiple linear regression method (as for temperature) to include also the information from SSS.

In order to take into account the higher resolution of the different SST fields two main sets of tests have been performed, from which higher resolution ARMOR3D-MESCLA experimental products have been obtained. The first one consisted in estimating the 3-D fields using the new SST input on the core $1/3^\circ$ Mercator horizontal grid. These tests required the remapping of each SST product on the $1/3^\circ$ grid (i.e. sub-sampling), which was performed using a bilinear interpolation of the four nearest points. The second test consisted in computing the 3-D field on each SST native grid ($1/4^\circ$, $1/10^\circ$ and $1/20^\circ$, respectively). The latter required the computation of the altimeter SLA grid on each SST grid (i.e. upsizing/interpolating the original data). Actually, upsizing has to be performed with particular care in order not to introduce spurious signal. After having

tested different methods (simple bilinear interpolation, Akima spline), a classical spline method has been chosen.

4.1.2 mEOF-Reconstruction

The multivariate EOF reconstruction (mEOF-R) technique is based on the analysis of the “multicoupled” variability of salinity, temperature and steric height profiles through a multivariate EOF decomposition and on the availability of corresponding surface values (Buongiorno Nardelli and Santoleri, 2005).

Here, we will briefly recall how mEOF-R works. A single $3m \times n$ multivariate observation matrix \mathbf{X} is obtained from the three original sets of data, each of $m \times n$ dimensions, where n is the number of measurements (stations) and m the number of vertical levels. Data are preliminarily normalized dividing each parameter by its standard deviation (computed for the whole profile). Mean profiles estimated from the whole training dataset are removed in order to obtain anomalies and estimate the covariances. The columns of this matrix consist of the three normalized profiles of T , S and SH anomalies, each taken at the same location.

$$\mathbf{X} = \begin{bmatrix} T(0, r_1) & T(0, r_2) & \dots & T(0, r_n) \\ \vdots & \vdots & \dots & \vdots \\ T(z_m, r_1) & T(z_m, r_2) & \dots & T(z_m, r_n) \\ S(0, r_1) & S(0, r_2) & \dots & S(0, r_n) \\ \vdots & \vdots & \dots & \vdots \\ S(z_m, r_1) & S(z_m, r_2) & \dots & S(z_m, r_n) \\ SH(0, r_1) & SH(0, r_2) & \dots & SH(0, r_n) \\ \vdots & \vdots & \dots & \vdots \\ SH(z_m, r_1) & SH(z_m, r_2) & \dots & SH(z_m, r_n) \end{bmatrix}$$

To compute the multivariate EOF, the Singular Value Decomposition of this new matrix of data is performed. In that way, “multi-coupled” modes are identified, each containing

High resolution mapping of 3-D mesoscale dynamics

B. Buongiorno Nardelli et al.

Title Page

Abstract

Introduction

Conclusions

References

Tables

Figures

⏪

⏩

◀

▶

Back

Close

Full Screen / Esc

Printer-friendly Version

Interactive Discussion



the three patterns corresponding to the parameters considered. $T(z, r)$, $S(z, r)$ and $SH(z, r)$ can thus be expanded in terms of these three series of patterns. The same coefficient/amplitude (a_k) is found for all parameters, L_k , M_k and N_k being the modes:

$$S(z, r) = \sum_{k=1}^n a_k(r)M_k(z)$$

$$S(z, r) = \sum_{k=1}^n a_k(r)M_k(z)$$

$$T(z, r) = \sum_{k=1}^n a_k(r)L_k(z)$$

If these expansions are limited to the first three modes, the vertical profiles can be estimated from the surface values ($z = 0$) of the three parameters solving the system for a_1 , a_2 and a_3 and substituting them in the truncated expansions:

$$\begin{cases} a_1(r)L_1(0) + a_2(r)L_2(0) + a_3(r)L_3(0) = T(0, r) \\ a_1(r)M_1(0) + a_2(r)M_2(0) + a_3(r)M_3(0) = S(0, r) \\ a_1(r)N_1(0) + a_2(r)N_2(0) + a_3(r)N_3(0) = SH(0, r) \end{cases}$$

Of course, it is also possible to truncate the expansions to the second mode, which actually means that only two surface parameters are sufficient to retrieve the whole profiles. Similarly, the whole analysis can be performed directly on two sets of parameter.

The *mEOF-R* method requires a training dataset of T , S and SH profiles to extract the main vertical modes of (co)variability. This training dataset might be selected differently at each grid point on the basis of different criteria: fixing a space and/or time search radius (e.g. 1000, week, month, year), keeping only the nearest n profiles, etc. Depending on this choice, one may end up with different reconstruction models (i.e.

High resolution mapping of 3-D mesoscale dynamics

B. Buongiorno Nardelli et al.

Title Page

Abstract

Introduction

Conclusions

References

Tables

Figures

⏪

⏩

◀

▶

Back

Close

Full Screen / Esc

Printer-friendly Version

Interactive Discussion



different mEOFs) for each grid point or with a single set of modes. After some preliminary hindcast tests (not shown), it was decided to select all the profiles collected in the domain within a monthly window. Given the sparse, even though regular, distribution of data in the *training* set, this was found to be the simplest but also most reliable way to estimate EOFs.

Similarly to the pre-processing performed by ARMOR3D, in order to retrieve the 3-D vertical fields from surface data, a preliminary step is to estimate/extract the surface steric heights from satellite altimeter data. Actually, as there is no way to evaluate the deeper baroclinic and the barotropic contributions from altimeter data and surface measurements alone, in a simple approximation, this estimation is reduced here to an adjustment of the ADT to minimize the differences between the steric height computed from simultaneous (or quasi-simultaneous) in situ profiles and co-located ADT estimates (through a simple regression). Differently to Guinehut et al. (2012), this adjustment has been performed here considering weekly matchups. The in situ *T/S* profiles described in Sect. 2 were re-interpolated at 10 dbar resolution down to 1000 dbar, and steric height profiles were obtained taking 1000 dbar as reference pressure level. These data have been used as training dataset, while altimeter ADT data ODYSSEA SST L4 and MESCLA SSS L4 data were used as surface input in the test of the mEOF-R technique.

4.2 Vertical velocity estimation

Relatively intense vertical exchanges in the oceans are associated to the mesoscale structures. Nevertheless, vertical velocities are generally lower by a factor up to 10^4 than horizontal ones, and consequently they are not easily measured through direct observations (e.g. Klein and Lapeyre, 2009; Frajka-Williams et al., 2011). Various indirect methodologies have thus been proposed to estimate vertical velocity from observed density and geostrophic velocity fields. Though more complicated techniques such as the semi-geostrophic Omega equation (Viudez and Dritchel, 2004) have been proposed, the most used technique is based on the solution of the quasi-geostrophic

High resolution mapping of 3-D mesoscale dynamics

B. Buongiorno Nardelli et al.

Title Page

Abstract

Introduction

Conclusions

References

Tables

Figures



Back

Close

Full Screen / Esc

Printer-friendly Version

Interactive Discussion



(QG) Omega equation (e.g. Tintoré et al., 1991; Buongiorno Nardelli et al., 2001; Pascual et al., 2004; Ruiz et al., 2009), which has already been shown to give reasonable estimates of the vertical velocities compared to primitive equation models (Pinot et al., 1996).

In this work, the algorithm for the solution \mathbf{Q} vector formulation of the Omega equation (as originally developed at IMEDEA) was adapted to the specific products that are used/developed within MESCLA project. Actually, the Omega equation requires in input both the geostrophic field and the density stratification. The geostrophic currents have been estimated referencing the thermal wind estimates to the absolute surface altimeter velocities (when applied to observation-based products). Two reference levels for dynamic height computation are considered for models: the surface and 1000 m depth. The code is derived from the QG vorticity and thermodynamic equation (Hoskins et al., 1978):

$$\nabla^2 (N^2 w) + f^2 \frac{\partial^2 w}{\partial z^2} = 2 \nabla \cdot \mathbf{Q}$$

$$\mathbf{Q} = \left[f \left(\frac{\partial V}{\partial x} \frac{\partial U}{\partial z} + \frac{\partial V}{\partial y} \frac{\partial V}{\partial z} \right), -f \left(\frac{\partial U}{\partial x} \frac{\partial U}{\partial z} + \frac{\partial U}{\partial y} \frac{\partial V}{\partial z} \right) \right]$$

where (U, V) are the geostrophic velocity components, N is the Brunt-Väisälä frequency and f the Coriolis parameter. In this implementation, N only depends on depth. Different boundary conditions have been tested (i.e. Dirichelet and Neumann conditions), however, given the elliptic nature of the Omega equation, no significant differences were found a few grid points away from the boundaries in the two cases.

High resolution mapping of 3-D mesoscale dynamics

B. Buongiorno Nardelli et al.

Title Page

Abstract

Introduction

Conclusions

References

Tables

Figures



Back

Close

Full Screen / Esc

Printer-friendly Version

Interactive Discussion



5 Results

5.1 Preliminary hindcast evaluation of the mEOF-R methods

Various mEOF-R products obtained from different configurations have been compared, and a first estimate of their accuracy has been estimated through a hindcast validation.

This means that the surface values of the in situ profiles used as training datasets were taken as input data for the reconstruction. The hindcast errors were thus estimated as the mean and standard deviation of the differences between the vertically reconstructed (synthetic) profiles and the original measurements. The advantage of this kind of validation is given by the large number of profiles available, while the disadvantage clearly resides in the fact that hindcast is not an independent validation, as the same data are used to train and test the method.

The hindcast validation was applied to the mEOF-R configurations listed below:

1. mEOF-r(T - S -SH). The mEOFs are computed from T , S and SH profiles and corresponding synthetic profiles are obtained using SST, SSS and SSH as input data (the amplitude of the first 3 modes is retrieved).
2. mEOF-r(T - S -SH)_{SST-SSH}. The mEOF are computed from T , S and SH profiles and corresponding synthetic profiles are obtained using only SST and SSH as input data (the amplitude of the first 2 modes is retrieved).
3. mEOF-r(T - S -SH)_{SSS-SSH}. The mEOF are computed from T , S and SH profiles and corresponding synthetic profiles are obtained using only SSS and SSH as input data (the amplitude of the first 2 modes is retrieved).
4. mEOF-r(T -SH). The mEOF are computed from T and SH profiles only, and corresponding synthetic profiles are obtained using SST and SSH as input data (the amplitude of the first 2 modes is retrieved).

High resolution mapping of 3-D mesoscale dynamics

B. Buongiorno Nardelli et al.

Title Page

Abstract

Introduction

Conclusions

References

Tables

Figures

⏪

⏩

◀

▶

Back

Close

Full Screen / Esc

Printer-friendly Version

Interactive Discussion



5. mEOF-r(S -SH). The mEOF are computed from S and SH profiles only, and corresponding synthetic profiles are obtained using SSS and SSH as input data (the amplitude of the first 2 modes is retrieved).

Mean Bias Error (MBE) and Standard Deviation Error (STDE) profiles for both temperature and salinity are shown in Fig. 1a and b, respectively. It is interesting to observe that the synthetic mEOF-r MBE is generally quite small. The mEOF-r provides the smallest STDE errors when only two modes are considered, both in the trivariate formulation and in the bivariate one.

A simple explanation for this may be given by analyzing the mEOF modes (Fig. 2) and corresponding explained covariance percentage. Similarly to what was found by Buongiorno Nardelli et al. (2006), the first mode is almost certainly driven by the quasi-geostrophic dynamics, as the SH pattern closely resembles the typical shape of the first baroclinic mode. However, even if this first mode explains an extremely high percentage of the variance (almost 99%), while only about 0.3% of it is explained by the second mode, some important information is still contained in the second mode. In fact, we also run a single mode mEOF(T - S -SH) reconstruction (both for temperature and salinity) which gave much worse results than the mEOF-r in the two mode configurations (see Fig. 3). Actually, T and S patterns in the first mEOF mode have the same sign, meaning that the surface anomalies with respect to the mean profile driven by this mode reflect down to the deep layers. On the opposite, the second mode basically accounts for the presence of T and S anomalies only in the upper layers, which might, for example, be related to the presence/absence of waters of coastal/riverine origin. More investigations will be needed to better understand which process drives the variability of this second mode. Meanwhile, it is clear that the third mode is related to conditions that apply to an extremely low number of profiles. Adding it to the reconstruction, in fact, leads to typical errors associated with an over-fitting of the data. Only the best performing techniques, as evaluated with the previous hindcast validation, have been applied to the SST, SSS and adjusted ADT maps. The selected techniques are the mEOF-r(T - S -SH)_{SST-SSH} and mEOF-r(T - S -SH)_{SSS-SSH}.

5.2 Combined ARMOR3D, synthetic ARMOR3D and mEOF-R comparison

A preliminary evaluation of the accuracy of combined and synthetic standard ARMOR3D products, new high resolution synthetic ARMOR3D products and new mEOF-R has been roughly estimated via a weekly matchup comparison, which means that the in situ profiles collected in a temporal range of ± 3 days (weekly matchups) have been taken aside as an independent test dataset, and have been compared with the co-located profiles obtained with the different reconstruction methods. The same matchup has been applied to eight different versions of the ARMOR3D product (see Sect. 4.1.1), as listed below:

1. Combined ARMOR3D (MERCATOR $1/3^\circ$ grid),
2. Synthetic ARMOR3D (MERCATOR $1/3^\circ$ grid – sub-sampled Reynolds SST),
3. Synthetic ARMOR3D (MERCATOR $1/3^\circ$ grid – sub-sampled Odyssea SST),
4. Synthetic ARMOR3D (MERCATOR $1/3^\circ$ grid – sub-sampled OSTIA SST),
5. Synthetic ARMOR3D (Reynolds SST on original $1/4^\circ$ grid),
6. Synthetic ARMOR3D (Odyssea SST on original $1/10^\circ$ grid),
7. Synthetic ARMOR3D (OSTIA SST on original $1/20^\circ$ grid),
8. Synthetic ARMOR3D (MESCLA HR SSS on original $1/10^\circ$ grid).

The matchup comparison has the advantage of starting from fully independent surface input data, but the number of in situ profiles available within this weekly window was also quite low (actually, 13 matchups were found, see Fig. 4), so that the estimated MBE and STDE may only give an indication on the methods' performance, while a longer test period should be used to get a real validation. Moreover, the estimated difference can possibly also be affected by the temporal variability at scales shorter than 3 days, which might not be negligible in rapidly evolving frontal areas.

High resolution mapping of 3-D mesoscale dynamics

B. Buongiorno Nardelli et al.

Title Page

Abstract

Introduction

Conclusions

References

Tables

Figures

⏪

⏩

◀

▶

Back

Close

Full Screen / Esc

Printer-friendly Version

Interactive Discussion



5 grids have very similar resolution at these latitudes) and Ostia SST, as Ostia SST effectively resolves structures at much larger scales than its nominal resolution ($1/20^\circ$). Similarly, the mEOF-R temperature fields at depth present quite different and smaller scale structures with respect to those obtained with the synthetic ARMOR3D products calculated from Reynolds and OSTIA. mEOF-r temperature at 100 m also displays slightly smaller scale structure and more intense gradients than those from synthetic ARMOR3D Odyssey. Concerning the salinity field, it has to be stressed that MESCLA HR-SSS and the ARMOR3D SSS fields computed from the first guess and covariances at the surface between altimeter SLA and salinity are quite different (Fig. 6b). In particular, the MESCLA HR-SSS field shows a very sharp gradient along the front of the Gulf Stream with much fresher SSS than those present in the ARMOR3D field. Both the mEOF-r and the ARMOR3D salinity reconstruction methods propagate this sharp gradient and the small scale structures retrieved by MESCLA HR SSS down to 100 m.

5.3 Comparison of the MyOcean model PE and QG vertical velocities

15 A comparison of the QG-vertical velocities (qgw) obtained by applying the Omega equation to Mercator model output with corresponding primitive equation solutions has been performed. The impact of the spatial and temporal resolution on the vertical velocity estimation has been assessed and the sensitivity to the choice of the reference level on the geostrophic and ageostrophic (vertical component) velocities have also been investigated. As for Sect. 5.2, all the plots refer to 100 m depth, which is a particularly interesting level as it corresponds approximately to the base of the euphotic layer in the Gulf Stream area (Oschlies and Garçon, 1998).

25 The different dynamic height patterns and corresponding Omega estimates show a high sensitivity, both in terms of shape and intensity, to the spatial resolution of the model (Fig. 7). Vertical velocities obtained from the $1/12^\circ$ (PSY2w) model (Fig. 7c–d) are a factor of 2–3 larger than the $1/4^\circ$ (PSY3w) (Fig. 7a–b) version (maximum upward and downward velocities of the order of $40\text{--}60\text{ m day}^{-1}$ vs. $20\text{--}30\text{ m day}^{-1}$, respectively). On the other hand, the comparison between PE and QG vertical velocities

High resolution mapping of 3-D mesoscale dynamics

B. Buongiorno Nardelli et al.

Title Page

Abstract

Introduction

Conclusions

References

Tables

Figures



Back

Close

Full Screen / Esc

Printer-friendly Version

Interactive Discussion



shows a reasonable agreement in both model simulations, even if model QG's values underestimate the PE velocities at low resolution (Fig. 7). These differences can be better quantified looking at the scatter plot and computing correlation coefficients, as displayed in Fig. 8 (similar results were also found for deeper layers, not shown). In fact, QG velocities displayed maximum upward and downward values of the order of 40–60 m day⁻¹ and 10–15 m day⁻¹, in the high resolution and low resolution tests, with correlation with PE (Pearson coefficient) reaching almost 0.8 and 0.7, respectively.

The results indicate that resolution is a key factor in the estimate of the vertical component of the ageostrophic velocity through the quasi-geostrophic omega (compared to PE estimates). If sufficient resolution is kept, velocities are more correctly reproduced even in the quasi-geostrophic approximation and, even though the patterns in the QG solution may slightly be smoother, the estimated values compare reasonably well. In the following, the QG method will thus be applied to the observation-based experimental 3-D products, providing a fully observational estimate of the vertical velocities over the Gulf Stream area.

5.4 Vertical velocities estimates from experimental 3-D products

Similarly to what was found for the tracer fields in Sect. 5.2, very similar *qgw* estimates were obtained from the synthetic experimental ARMOR3D using the SST L4 sub-sampled on the 1/3° Mercator grid (not shown). Conversely, vertical velocity intensity increased significantly when experimental synthetic ARMOR3D fields were computed on the (higher) original SST grid resolution and with mEOFr. A qualitative comparison of the vertical velocities retrieved by applying the Omega equation to the synthetic ARMOR3D products (listed as 4–8 in Sect. 5.2) and mEOF-r field is thus illustrated in Fig. 9. The lowest velocities were estimated from the synthetic ARMOR3D using the Reynolds L4 SST (peak *qgw* ~32 m day⁻¹, horizontal velocities peak ~1.5 m s⁻¹). Coherently with the findings of the Sect. 5.2, synthetic ARMOR3D *qgw* from OSTIA, though having the highest nominal resolution, do not display the highest average and peak velocities, though they are still significantly higher than those obtained

High resolution mapping of 3-D mesoscale dynamics

B. Buongiorno Nardelli et al.

Title Page

Abstract

Introduction

Conclusions

References

Tables

Figures



Back

Close

Full Screen / Esc

Printer-friendly Version

Interactive Discussion



climatologies or sparse observations of temperature, salinity or velocities. On the other hand, the limits of present observation-based products are correctly identified in their relatively low resolution and by the difficulties to provide any estimate of the ocean currents beyond the geostrophic approximation.

5 Within the MyOcean R&D project MESCLA, a step towards a more efficient combination and more complex analysis of existing observations has been made. MESCLA tested innovative methods for the high resolution mapping of 3-D mesoscale dynamics from a combination of in situ and satellite data (as described in Sect. 4.1), developing
10 new products that might be used as prototypes to gradually build the next generations of operational observation-based products. In order to demonstrate the new techniques' potential, different estimates of the vertical velocities derived from different 3-D synthetic fields through a quasi-geostrophic diagnostic model have been compared (Sect. 5). Resolution confirmed to be an important factor for the retrieval of the currents. However, even in the limits of a simplified dynamical framework, and knowing
15 that most of the analysis could not necessarily go beyond a simple qualitative comparison (vertical velocities cannot be measured directly at sea), realistic estimates of the vertical field could be retrieved, at least as compared to those diagnosed through primitive equation numerical models. The ocean observation-based products tested within MESCLA might thus open a wide range of possible applications for both Operational
20 Oceanography and Ocean Climate Monitoring studies.

Acknowledgements. This work was carried out in the framework of the MESCLA (MEsoSCaLe dynamical Analysis) project, funded within the *MyOcean Call for R&D Proposals* (2010–2012, Mercator Ocean Ref. PB-LC 10-103). MyOcean project (Development and pre-operational validation of GMES Marine Core Services (2009–2012) has been funded within the call EU FP7-
25 SPACE-2007-1 (Grant Agreement no. 218812).

High resolution mapping of 3-D mesoscale dynamics

B. Buongiorno Nardelli et al.

Title Page

Abstract

Introduction

Conclusions

References

Tables

Figures



Back

Close

Full Screen / Esc

Printer-friendly Version

Interactive Discussion



References

- Allen, J. T. and Smeed, D. A.: Potential vorticity and vertical velocity at the Iceland-Færøes front, *J. Phys. Oceanogr.*, 26, 2611–2634, 1996.
- Autret, E. and Piollé, J. F.: Implementation of a global SST analysis, MERSEA-WP02-IFR-STR-001-1A report, 2007.
- AVISO: Ssalto/Duacs userHandbook: (M)SLAand(M)ADT near-real time and delayed time products, SALP-MU-P-EA-21065-CLS ed. 2.6, 67 pp., 2011.
- Barnier, B., Madec, G., Penduff, T., Molines, J. M., Treguier, A. M., Le Sommer, J., Bekmann, A., Biastoch, A., Boning, C., Dengg, J., Derval, C., Durand, E., Gulev, S., Remy, E., Talandier, C., Theeten, S., Maltrud, M., McClean, J., and De Cuevas, B.: Impact of partial steps and momentum advection schemes in a global ocean circulation model at eddy-permitting resolution, *Ocean Dynam.*, 56, 543–567, 2006.
- Bretherton, F. P., Davis, R. E., and Fandry, C. B.: A technique for objective analysis and design of oceanographic experiments applied to MODE-73, *Deep-Sea Res. I*, 23, 559–582, 1976.
- Buongiorno Nardelli, B.: A novel approach to the high resolution interpolation of in situ Sea Surface Salinity, *J. Atmos. Oceanic Technol.*, in review, 2012.
- Buongiorno Nardelli, B. and Santoleri, R.: Reconstructing synthetic profiles from surface data, *J. Atmos. Ocean. Tech.*, 21, 693–703, 2004.
- Buongiorno Nardelli, B. and Santoleri, R.: Methods for the reconstruction of vertical profiles from surface data: multivariate analyses, residual GEM and variable temporal signals in the North Pacific Ocean, *J. Atmos. Ocean. Tech.*, 22, 1763–1782, 2005.
- Buongiorno Nardelli, B., Sparnocchia, S., Santoleri, R.: Small mesoscale features at a meandering upper ocean front in the western Ionian Sea (Mediterranean Sea): vertical motion and potential vorticity analysis, *J. Phys. Oceanogr.*, 31, 2227–2250, 2001.
- Buongiorno Nardelli, B., Cavalieri, O., Rio, M.-H., Santoleri, R.: Subsurface geostrophic velocities inference from altimeter data: application to the Sicily Channel (Mediterranean Sea), *J. Geophys. Res.*, 111, C04007, doi:10.1029/2005JC003191, 2006.
- Carnes, M. R., Teague, W. J., and Mitchell, J. L.: Inference of subsurface thermohaline structure from fields measurable by satellite, *J. Atmos. Ocean. Tech.*, 11, 551–566, 1994.
- Dash, P., Ignatov, A., Kihai, Y., and Sapper, J.: The SST Quality Monitor (SQUAM), *J. Atmos. Ocean. Tech.*, 27, 1899–1917, doi:10.1175/2010JTECHO756.1, 2010.

OSD

9, 1045–1083, 2012

High resolution mapping of 3-D mesoscale dynamics

B. Buongiorno Nardelli et al.

Title Page

Abstract

Introduction

Conclusions

References

Tables

Figures

⏪

⏩

◀

▶

Back

Close

Full Screen / Esc

Printer-friendly Version

Interactive Discussion

High resolution mapping of 3-D mesoscale dynamics

B. Buongiorno Nardelli et al.

Title Page

Abstract

Introduction

Conclusions

References

Tables

Figures

◀

▶

◀

▶

Back

Close

Full Screen / Esc

Printer-friendly Version

Interactive Discussion



- Dhomps, A. -L., Guinehut, S., Le Traon, P.-Y., and Larnicol, G.: A global comparison of Argo and satellite altimetry observations, *Ocean Sci.*, 7, 175–183, doi:10.5194/os-7-175-2011, 2011.
- Dombrowsky, E., Bertino, L., Brassington, G. B., Chassignet, E. P., Davidson, F., Hurlburt, H. E., Kamachi, M., Lee, T., Martin, M. J., Mei, S., and Tonani, M.: GODAE systems in operation, *Oceanography*, 22, 80–95, doi:10.5670/oceanog.2009.68, 2009.
- Donlon, C. J., Casey, K. S., Robinson, I. S., Gentemann, C. L., Reynolds, R. W., Barton, I., Arino, O., Stark, J., Rayner, N., Le Borgne, P., Poulter, D., Vazquez-Cuervo, J., Armstrong, E., Beggs, H., Llewellyn-Jones, D., Minnett, P. J., Merchant, C. J., and Evans, R.: The GODAE High Resolution Sea Surface Temperature Pilot Project, *Oceanography*, 22, 34–45, 2009.
- Farneti, R., Delworth, T. L., Rosati, A. J., Griffies, S. M., and Zeng, F.: The Role of Mesoscale Eddies in the Rectification of the Southern Ocean Response to Climate Change, *J. Phys. Oceanogr.*, 40, 1539–1557, doi:10.1175/2010JPO4353.1, 2010.
- Fox, D. N., Teague, W. J., Barron, C. N., Carnes, M. R., and Lee, C. M.: The modular ocean data assimilation system (MODAS), *J. Atmos. Ocean. Tech.*, 19, 240–252, 2002.
- Frajka-Williams, E., Eriksen, C. C., Rhines, P. B., and Harcourt, R. R.: Determining Water Velocities from Seaglider, *J. Atmos. Ocean. Tech.*, doi:10-1175/2011JTECHO830.1, 2011.
- Gavart, M. and De Mey, P.: Isopycnal EOFs in the Azores Current region: A statistical tool for dynamical analysis and data assimilation, *J. Phys. Ocean.*, 27, 2146–2157, 1997.
- Gruber, N., Lachkar, Z., Frenzel, H., Marchesiello, P., Munnich, M., McWilliams, J. C., Nagai, T., and Plattner, G.: Mesoscale eddy-induced reduction of biological production in eastern boundary upwelling systems, *Nature Geosci.*, 4, 787–792, doi:10.1038/ngeo1273, 2011.
- Guinehut, S., Le Traon, P. Y., Larnicol, G., and Philipps, S.: Combining Argo and remote-sensing data to estimate the ocean three-dimensional temperature fields - a first approach based on simulated observations, *J. Mar. Sys.*, 46, 85–98, 2004.
- Guinehut, S., Le Traon, P.-Y., and Larnicol, G.: What can we learn from Global Altimetry/Hydrography comparisons ?, *Geophys. Res. Lett.*, 33, L10604, doi:10.1029/2005GL025551, 2006.
- Guinehut, S., Dhomps, A.-L., Larnicol, G., and Le Traon, P.-Y.: High Resolution 3D temperature and salinity fields derived from in situ and satellite observations, *Ocean Sci. Discuss.*, in press, 2012.
- Hoskins, B. J., Draghici, I., and Davies, H. C.: A new look at the omega-equation, *Q. J. Roy. Meteorol. Soc.*, 104, 31–38, 1978.

High resolution mapping of 3-D mesoscale dynamics

B. Buongiorno Nardelli et al.

Title Page

Abstract

Introduction

Conclusions

References

Tables

Figures

⏪

⏩

◀

▶

Back

Close

Full Screen / Esc

Printer-friendly Version

Interactive Discussion



- Ingleby, B. and Huddleston, M.: Quality control of ocean temperature and salinity profiles – historical and real-time data. *J. Mar. Sys.*, 65, 158–175, doi:10.1016/j.jmarsys.2005.11.019, 2007.
- 5 Klein, P. and Lapeyre, G.: The oceanic vertical pump induced by mesoscale eddies, *Annu. Rev. Marine. Sci.*, 1, 351–375, 2009.
- Larnicol, G., Guinehut, S., Rio, M.-H., Drevillon, M., Faugere, Y., and Nicolas, G.: The Global Observed Ocean Products of the French Mercator project, *Proceedings of 15 Years of progress in Radar Altimetry Symposium*, ESA Special Publication, SP-614, 2006.
- 10 Lellouche, J.-M., Le Galloudec, O., Dréville, M., Régnier, C., Greiner, E., Garric, G., Ferry, N., Desportes, C., Testut, C. E., Bricaud, C., Bourdallé-Badie, R., Tranchant, B., Drillet, Y., Daudin, A., and De Nicola, C.: Evaluation of real time and future monitoring and forecasting systems at Mercator Océan, OS, *Ocean Sci. Discuss.*, in press, 2012.
- Lévy, M.: The modulation of biological production by oceanic mesoscale turbulence, *Lect. Notes Phys.*, 744, 219–261, *Transport in Geophysical flow: Ten years after*, edited by: Weiss, J. B. and Provenzale, A., Springer, 2008.
- 15 Madec, G.: “NEMO ocean engine”, *Note du Pole de modélisation*, Institut Pierre-Simon Laplace (IPSL), France, No. 27, ISSN No 1288-1619, 2008.
- Maturi, E., Harris, A., and Sapper, J.: A New Ultra High Resolution Sea Surface Temperature Analyses from GOES-R and NPOESS-VIIRS, 90th AMS Annual Meeting, 6th Annual Symposium on Future National Operational Environmental Satellite Systems-NPOESS and GOES-R, 17–21 January 2010, Atlanta, Georgia, 2010.
- 20 Meinen, C. S. and Watts, D. R.: Vertical structure and transport on a transect across the North Atlantic Current near 42 degrees N: time series and mean, *J. Geophys. Res.*, 105, 21869–21891, 2000.
- 25 Mitchell, D. A., Wimbush, M., Watts, D. R., and Teague, W. J.: The Residual GEM technique and its application to the Southwestern Japan/East Sea, *J. Atmos. Ocean. Tech.*, 21, 1895–1909, 2004.
- Mulet, S., Rio, M.-H., Mignot, A., Guinehut, S., and Morrow, R.: A new estimate of the global 3D geostrophic ocean circulation based on satellite data and in situ measurements, *Deep Sea Res. II*, accepted, 2012.
- 30 Oschlies, A. and Garçon, V.: Eddy-induced enhancement of primary production in a model of the North Atlantic Ocean, *Nature*, 394, 266–269, 1998.

High resolution mapping of 3-D mesoscale dynamics

B. Buongiorno Nardelli et al.

Title Page

Abstract

Introduction

Conclusions

References

Tables

Figures

⏪

⏩

◀

▶

Back

Close

Full Screen / Esc

Printer-friendly Version

Interactive Discussion



- Pascual, A. and Gomis, D.: Use of Surface Data to Estimate Geostrophic Transport, *J. Atmos. Ocean. Tech.*, 20, 912–926, 2003.
- Pascual, A., Gomis, D., Haney, R. H., and Ruiz, S.: A quasi-geostrophic analysis of a meander in the Palamós Canyon: vertical velocity, geopotential tendency and a relocation technique, *J. Phys. Oceanogr.*, 34, 2274–2287, 2004.
- Pinot, J.-M., Tintoré, J., and Wang, D.-P.: A study of the omega equation for diagnosing vertical motions at ocean fronts, *J. Mar. Res.*, 54, 239–259, 1996.
- Reynolds, R. W. and Chelton, D. B.: Comparisons of daily sea surface temperature analyses for 2007–08, *J. Climate*, 23, 3545–3562, 2010.
- Roemmich, D. and Gilson, J.: The 2004–2008 mean and annual cycle of temperature, salinity and steric height in the global ocean from the Argo program, *Prog Oceanogr.*, 82, 81–100, 2009.
- Ruiz, S., Pascual, A., Garau, B., Pujol, I., and Tintoré, J.: Vertical motion in the upper ocean from glider and altimetry data, *Geophys. Res. Lett.*, 36, L14607, doi:10.1029/2009GL038569, 2009.
- Stammer, D., Köhl, A., Awaji, T., Balmaseda, M., Behringer, D., Carton, J., Ferry, N., Fischer, A., Fukumori, I., Giese, B., Haines, K., Harrison, E., Heimbach, P., Kamachi, M., Keppenne, C., Lee, T., Masina, S., Menemenlis, D., Ponte, R., Remy, E., Rienecker, M., Rosati, A., Schröter, J., Smith, D., Weaver, A., Wunsch, C., and Xue, Y.: Ocean Information Provided through Ensemble Ocean Syntheses, in: *Proceedings of OceanObs'09: Sustained Ocean Observations and Information for Society*, edited by: Hall, J., Harrison, D. E., and Stammer, D., Vol. 2, Venice, Italy, 21–25 September 2009, ESA Publication WPP-306, 2010.
- Tintoré, J., Gomis, D., Alonso, S., and Parrilla, G.: Mesoscale dynamics and vertical motion in the Alboran Sea, *J. Phys. Oceanogr.*, 21, 811–823, doi:10.1175/1520-0485(1991)021<0811:MDAVMI>2.0.CO;2, 1991.
- Tranchant, B., Testut, C. E., Renault, L., Ferry, N., Obligis, E., Boone, C., and Larnicol, G.: Data assimilation of simulated SSS SMOS products in an ocean forecasting system, *J. Operational Oceanogr.*, 1, 19–27, 2008.
- Viúdez, A. and Dritschel, D. G.: Potential Vorticity and the Quasigeostrophic and Semi-geostrophic Mesoscale Vertical Velocity, *J. Phys. Oceanogr.*, 34, 865–887, doi:10.1175/1520-0485(2004)034<0865:PVATQA>2.0.CO;2, 2004.
- Von Schuckmann, K., Gaillard, F., and Le Traon, P.-Y.: Global hydrographic variability patterns during 2003–2008, *J. Geophys. Res.*, 114, C09007, doi:10.1029/2008JC005237, 2009.

High resolution mapping of 3-D mesoscale dynamics

B. Buongiorno Nardelli et al.

Title Page

Abstract

Introduction

Conclusions

References

Tables

Figures

⏪

⏩

◀

▶

Back

Close

Full Screen / Esc

Printer-friendly Version

Interactive Discussion

Table 1. Description of the L4 SST products used.

SST	Spatial Res.	Time series available	Sensors	Method
Reynolds HR AVHRR-AMSR	1/4°	Since 2002/06/01	AVHRR + AMSR + in situ observations	Bias correction, Sea ice to SST conversion algorithm, First guess = previous analysis (Reynolds et al., 2007)
Ostia	1/20°	Since 2006/01/01	AATSR (Envisat), AMSR-E (Aqua), AVHRR-LAC (NOAA 17 & 18), AVHRR-GAC (NOAA 18), InSitu observations, Sea ice, primarily SSM/I (DMSP), SEVIRI (MSG1), TMI (TRMM).	Bias correction, First guess = previous analysis (Donlon et al., 2011)
Odyssea	1/10°	From 2007/10/01 to 2009/11/23	AATSR, AVHRR (NOAA 17 & 18), GOES/VISSR, MSG-1/SEVIRI; AMSRE, TMI	Sampling or averaging, First guess: reference daily climatology (Autret and Piollé, 2007)

High resolution mapping of 3-D mesoscale dynamics

B. Buongiorno Nardelli et al.

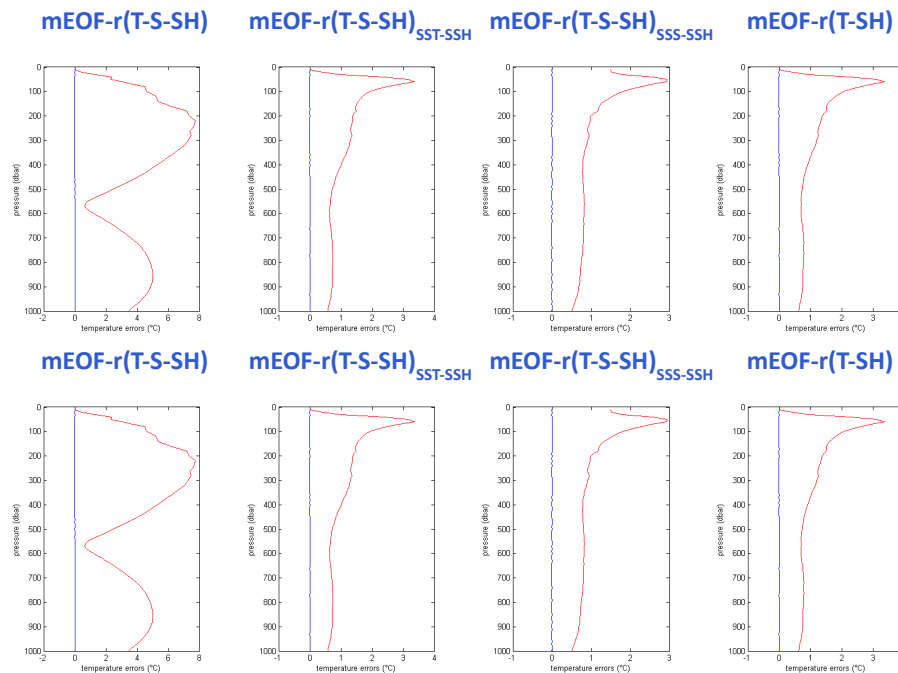


Fig. 1. (a) Hindcast temperature mean bias errors (blue) and standard deviation errors (red) for different configurations of the mEOF-r technique. (b) Hindcast salinity mean bias errors (blue) and standard deviation errors (red) for different configurations of the mEOF-r technique.

Title Page

Abstract

Introduction

Conclusions

References

Tables

Figures

⏪

⏩

◀

▶

Back

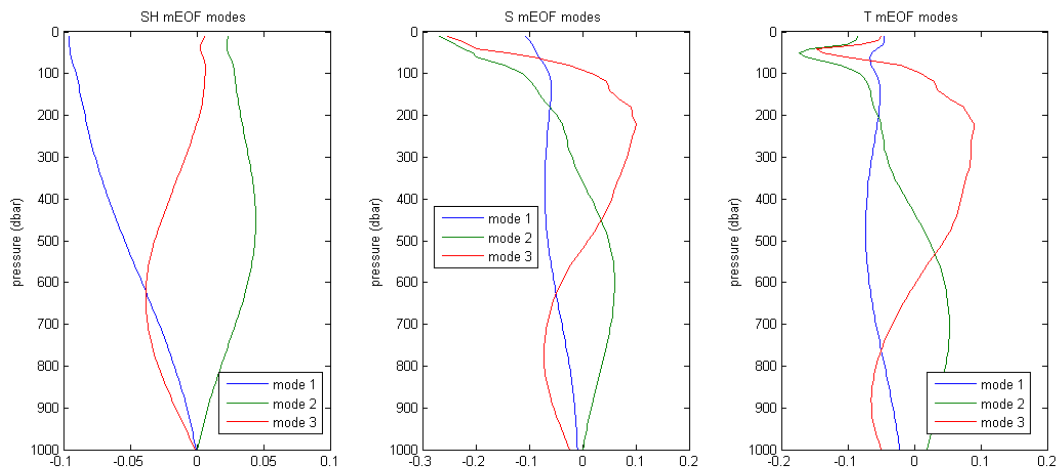
Close

Full Screen / Esc

Printer-friendly Version

Interactive Discussion

**High resolution
mapping of 3-D
mesoscale dynamics****B. Buongiorno Nardelli et
al.**

**Fig. 2.** Trivariate (*T-S-SH*) mEOF modes.[Title Page](#)[Abstract](#)[Introduction](#)[Conclusions](#)[References](#)[Tables](#)[Figures](#)[⏪](#)[⏩](#)[◀](#)[▶](#)[Back](#)[Close](#)[Full Screen / Esc](#)[Printer-friendly Version](#)[Interactive Discussion](#)

High resolution mapping of 3-D mesoscale dynamics

B. Buongiorno Nardelli et al.

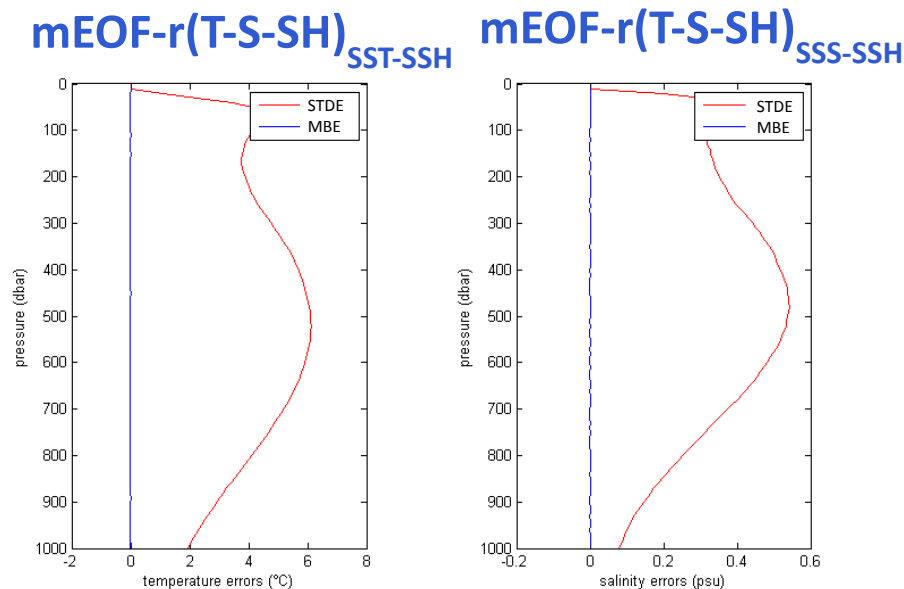


Fig. 3. Hindcast temperature and salinity mean bias errors (blue) and standard deviation errors (red) when using only the first mode in the mEOF-r trivariate reconstruction.

[Title Page](#)
[Abstract](#)
[Introduction](#)
[Conclusions](#)
[References](#)
[Tables](#)
[Figures](#)
[⏪](#)
[⏩](#)
[◀](#)
[▶](#)
[Back](#)
[Close](#)
[Full Screen / Esc](#)
[Printer-friendly Version](#)
[Interactive Discussion](#)

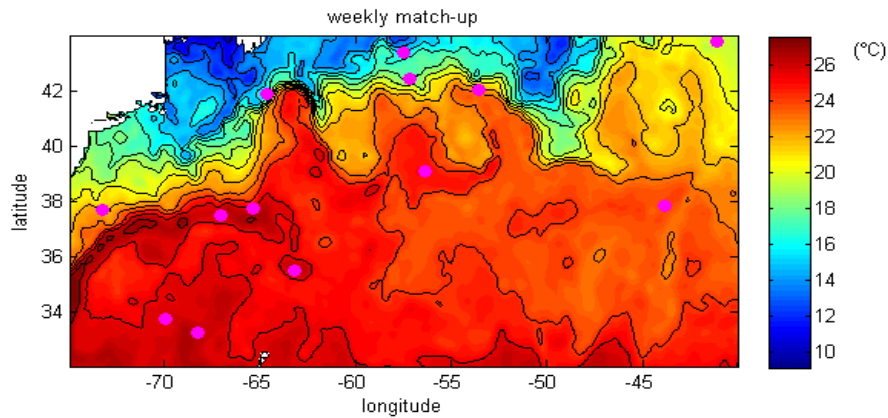


Fig. 4. Matchups location superimposed on 17 October 2007 Odyssea SST L4.

High resolution mapping of 3-D mesoscale dynamics

B. Buongiorno Nardelli et al.

Title Page	
Abstract	Introduction
Conclusions	References
Tables	Figures
⏪	⏩
◀	▶
Back	Close
Full Screen / Esc	
Printer-friendly Version	
Interactive Discussion	

High resolution mapping of 3-D mesoscale dynamics

B. Buongiorno Nardelli et al.

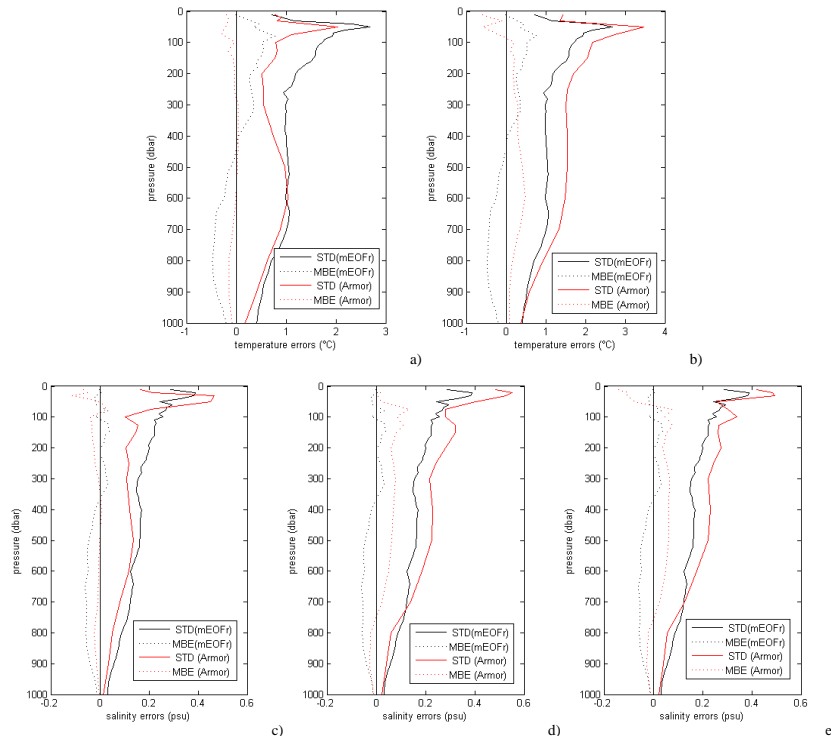


Fig. 5. Mean (dotted lines) and standard deviation (solid lines) of the difference between: – in situ temperature profiles and corresponding data from mEOF-r and combined ARMOR3D (**a**); in situ temperature profiles and corresponding data from mEOF-r and synthetic ARMOR3D using Odyssea SST (**b**); – in situ salinity profiles and corresponding data from mEOF-r and combined ARMOR3D (**c**); in situ salinity profiles and corresponding data from mEOF-r and synthetic ARMOR3D on Odyssea SST grid (**d**); in situ salinity profiles and corresponding data from mEOF-r and synthetic ARMOR3D using MESCLA SSS (**e**).

[Title Page](#)
[Abstract](#)
[Introduction](#)
[Conclusions](#)
[References](#)
[Tables](#)
[Figures](#)
[Back](#)
[Close](#)
[Full Screen / Esc](#)
[Printer-friendly Version](#)
[Interactive Discussion](#)

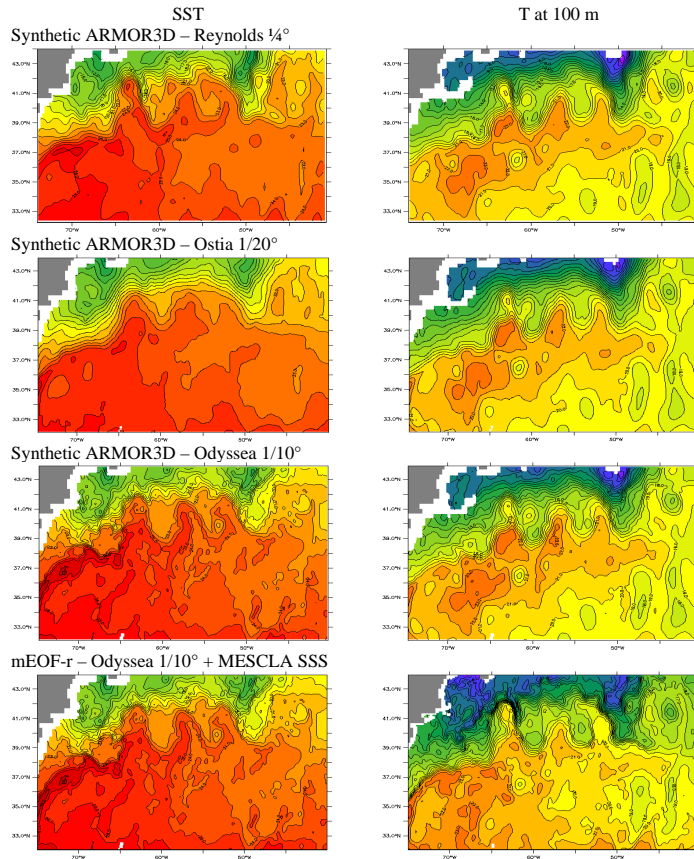


Fig. 6a. SST and temperature at 100 m from the four reconstruction methods selected (see details in the text). The color scale range from 0 to 30, every 1, in °C.

High resolution mapping of 3-D mesoscale dynamics

B. Buongiorno Nardelli et al.

Title Page

Abstract Introduction

Conclusions References

Tables Figures

⏪ ⏩

◀ ▶

Back Close

Full Screen / Esc

Printer-friendly Version

Interactive Discussion



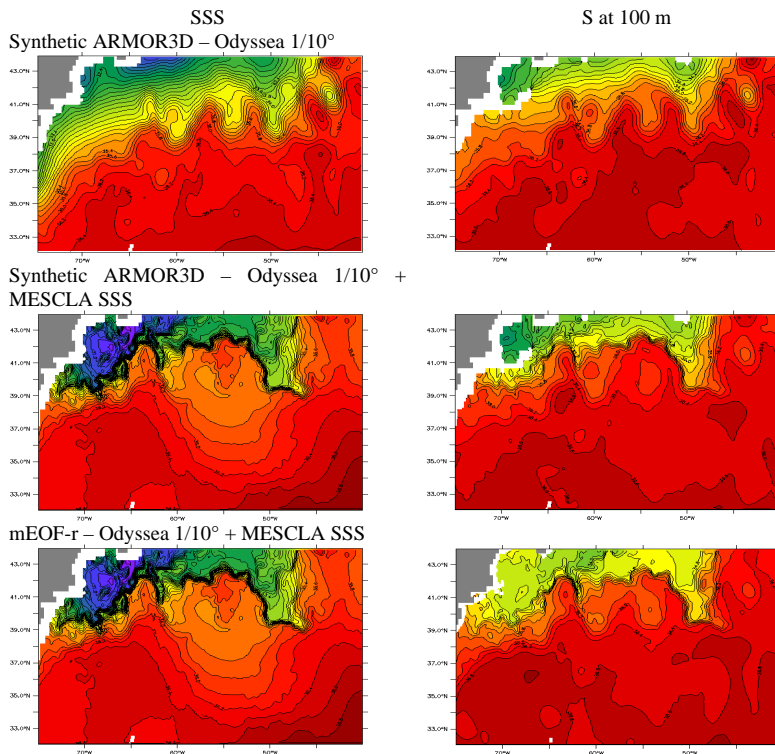


Fig. 6b. SSS and salinity at 100 m from the three reconstruction methods selected (see details in the text). The color scale range from 30 to 37, every 0.2 for the SSS and from 31 to 37, every 0.2 for the S at 100 m.

High resolution mapping of 3-D mesoscale dynamics

B. Buongiorno Nardelli et al.

Title Page

Abstract Introduction

Conclusions References

Tables Figures

⏪ ⏩

◀ ▶

Back Close

Full Screen / Esc

Printer-friendly Version

Interactive Discussion



High resolution mapping of 3-D mesoscale dynamics

B. Buongiorno Nardelli et al.

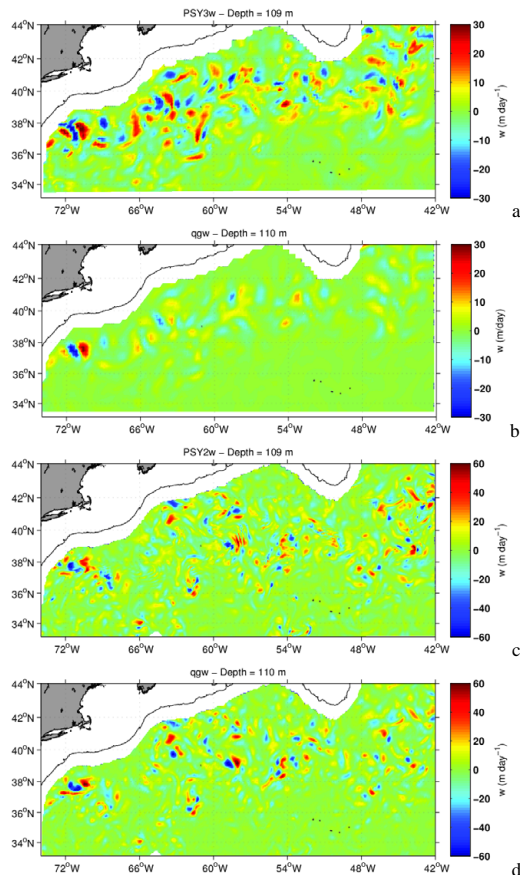


Fig. 7. Vertical velocity fields at 110 m as obtained from primitive equation and quasi-geostrophic Omega equation for PSY3 ($1/4^\circ$) and PSY2 ($1/12^\circ$) Mercator models.

[Title Page](#)
[Abstract](#)
[Introduction](#)
[Conclusions](#)
[References](#)
[Tables](#)
[Figures](#)
[Back](#)
[Close](#)
[Full Screen / Esc](#)
[Printer-friendly Version](#)
[Interactive Discussion](#)

High resolution mapping of 3-D mesoscale dynamics

B. Buongiorno Nardelli et al.

Title Page

Abstract

Introduction

Conclusions

References

Tables

Figures

◀

▶

◀

▶

Back

Close

Full Screen / Esc

Printer-friendly Version

Interactive Discussion

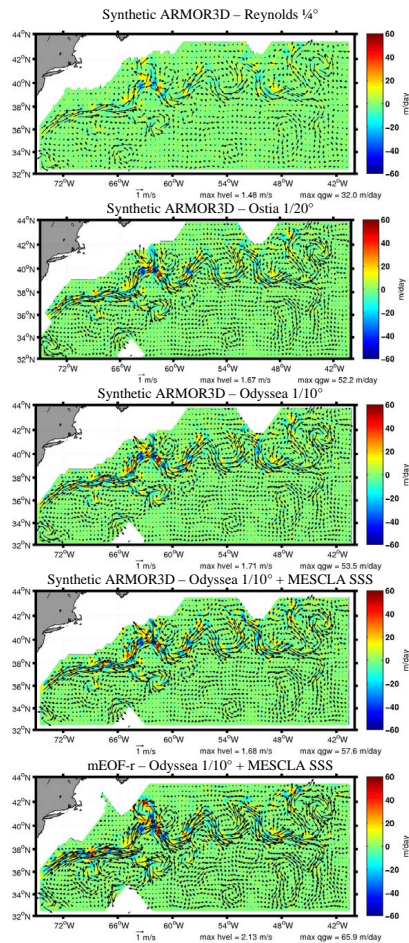


Fig. 9. QG vertical velocity fields at 100 m as retrieved from the synthetic ARMOR3D and mEOF-r fields.